The Canadian Mineralogist
Vol. 34, pp. 893-900 (1996)

THE THERMAL BEHAVIOR OF CANCRINITE

ISHMAEL HASSAN

Department of Geology, Faculty of Science, University of Kuwait, P.O. Box 5969, Safat, 13060, Kuwait

ABSTRACT

Differential thermal analyses were carried out on cancrinite from Bancroft, Ontario, ideal formula $Na_6Ca_2[Al_6Si_6O_{24}](CO_3)_2{\cdot}2H_2O$, using a Netzsch STA 409 EP/3/D Simultaneous TG–DTA apparatus. A finely powdered sample was heated from 20 to 1400°C. The thermal expansion coefficients, measured from the same cancrinite, and published separately, and XRD data are combined with the new data to give a complete description of the thermal behavior of cancrinite. The short Na1–H_2O(II) distance in the —H_2O(I)——Na1—H_2O(II)—— chain expands to equal the distance between adjacent H_2O molecules. This expansion causes the Na atoms to move toward the plane of the six-membered rings of tetrahedra and forces the tetrahedra to rotate, such that the rings become more planar. The Na1 atoms then form bonds to all six (O1 and O2) framework oxygen atoms. Although H_2O is lost continuously, the maximum losses of H_2O(I) and H_2O(II) are at 304 and 683°C, respectively. The supercell disappears at 868°C, and the maximum loss of CO_2 occurs at 949°C. A small amount of Cl_2 possibly is lost at 1066°C. The Na and Ca atoms are probably disordered at 1102°C, whereas the Al and Si atoms are probably disordered at 1199°C. Finally, melting of cancrinite occurs at 1255°C.

Keywords: cancrinite, thermal behavior, differential thermal analyses (DTA–TG), high-temperature powder X-ray diffraction.

SOMMAIRE

L'analyse thermique différentielle d'un échantillon de cancrinite provenant de Bancroft, en Ontario, et ayant comme formule idéale $Na_6Ca_2[Al_6Si_6O_{24}](CO_3)_2{\cdot}2H_2O$, a été complétée avec un appareil Netzsch STA 409 EP/3/D, réglé pour aussi obtenir des données thermogravimétriques. L'expérience a porté sur un échantillon pulvérisé et chauffé entre 20° et 1400°C. Les coefficients d'expansion thermique, mesurés sur le même échantillon et publiés ailleurs, les données de diffraction X et les nouvelles données mènent à une description complète du comportement thermique de la cancrinite. Les distances relativement courtes entre Na1 et H_2O(II) le long des chaînes —H_2O(I)——Na1—H_2O(II)—— s'allongent en chauffant pour équivaloir à la distance entre molécules d'eau adjacentes. Cet allongement a pour effet de déplacer les atomes de Na vers le plan d'anneaux de six tétraèdres, et force ces tétraèdres de se déplacer afin de rendre les anneaux davantage planes. Les atomes Na1 forment ainsi des liaisons avec les six atomes d'oxygène O1 et O2 de la trame. Quoique l'eau est libérée continuellement, les pertes maximales en H_2O(I) et H_2O(II) sont signalées à 304 et 683°C, respectivement. La surmaille disparaît à 868°C, et la perte maximale en CO_2 se situe à 949°C. Il est possible qu'une fraction du Cl_2 se volatilise à 1066°C. Les atomes Na et Ca deviennent désordonnés probablement à 1102°C, tandis que les atomes Al et Si deviennent désordonnés tout probablement à 1199°C. La cancrinite fond à 1255°C.

(Traduit par la Rédaction)

Mots-clés: cancrinite, comportement thermique, analyse thermique différentielle, diffraction X à température élevée, méthode des poudres.

INTRODUCTION

The structures of the cancrinite-group minerals are characterized by parallel six-membered rings consisting of alternating AlO_4 and SiO_4 tetrahedra. The hexagonal symmetry is the result of the stacking of such six-membered rings in an *ABAB...* sequence; this sequence leads to large continuous channels that are formed by twelve-membered rings of alternating AlO_4 and SiO_4 tetrahedra (Fig. 1a). The cancrinite structure also contains small ε-cages that occur along the three-fold axes (Fig. 1b). The ε-cages enclose $[Na{\cdot}H_2O]^+$ clusters, and the large channels contain the CO_3 groups and other Na and Ca cations (Na2; Fig. 1a). In the Na1 coordination in the cage, there is a long (I) and a short (II) Na1–H_2O distance in the —H_2O(I)——Na1—H_2O(II)—— chain [see Hassan (1996), and references therein). The H_2O molecules are disordered about the 3-fold axes because of hydrogen bonding (Grundy & Hassan 1982).

On heating, several steps are expected in the decomposition of cancrinite: (1) loss of CO_2, (2) loss of H_2O (I), (3) loss of H_2O (II), (4) loss of superstructure, and (5) melting. This study was carried out to

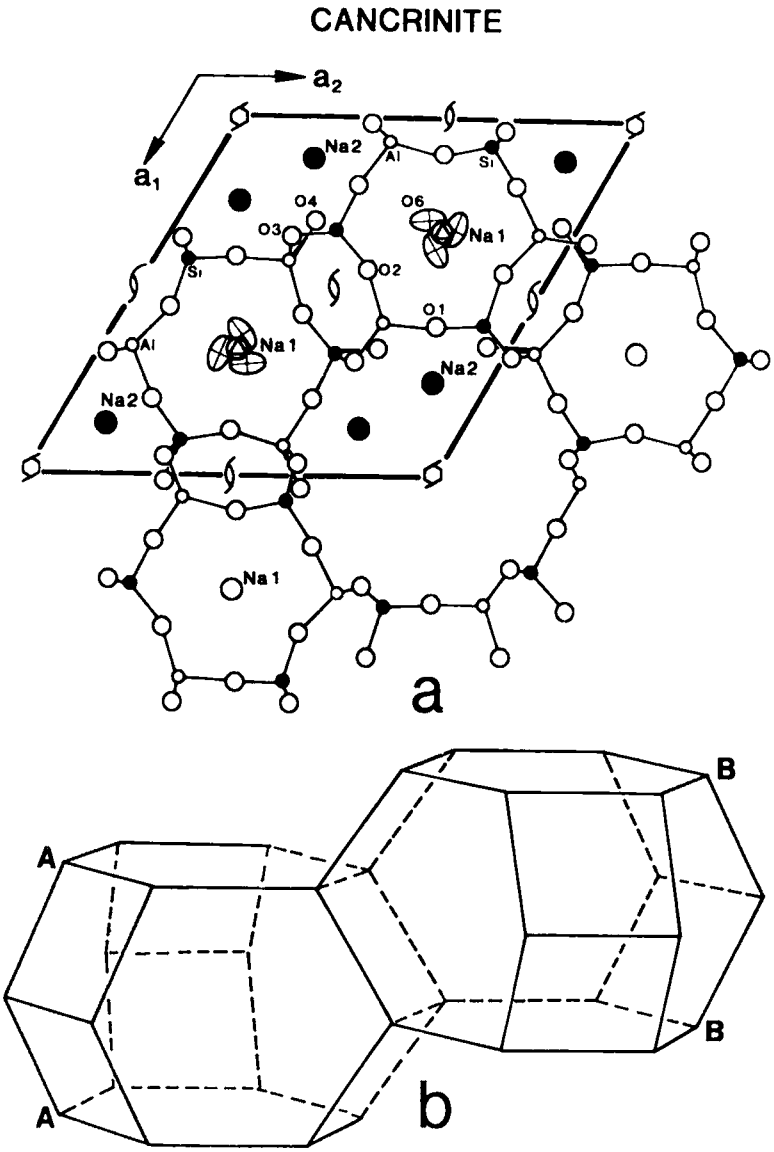

FIG. 1. (a) Crystal structure of cancrinite showing four-, six-, and twelve-membered rings of alternating silicon and aluminum tetrahedra (after Grundy & Hassan 1982). (b) Schematic illustration of the two ε-cages per unit cell in cancrinite.

determine the temperature at which each step occurs. Previously unpublished data obtained by high-temperature X-ray diffraction (XRD) (Hassan 1996) are combined with results of the present thermal analyses (DTA, TG, DDTA, and DTG) to give a complete description of the thermal behavior of cancrinite, as determined with a sample from Bancroft, Ontario. The chemical formula is $Na_{5.96}Ca_{1.52}[Al_6Si_6O_{24}](CO_3)_{1.57}{\cdot}1.75H_2O$ (Table 1). and the hexagonal subcell parameters are $a = 12.590$, $c = 5.117$ Å; the hexagonal supercell has as parameters $a \times 8c$ (= 40.936 Å; Grundy & Hassan 1982, Hassan & Buseck 1992). The chemical analyses indicate that H_2O, CO_2, and Cl_2 are important volatile constituents, which one would expect to be liberated on heating.

TABLE 1. CHEMICAL COMPOSITION OF CANCRINITE

Chemical Composition		Cell Contents †	
SiO_2 wt.%	34.35	Si	5.98
Al_2O_3	29.35	Al	6.02
Fe_2O_3	0.03	Fe	0.03
MgO	0.01	Mg	0.03
CaO	8.11	Ca	1.52
Na_2O	17.66	Na	5.96
K_2O	0.10	K	0.02
H_2O^+	3.02	H_2O	1.75
H_2O^-	0.11		
CO_2	6.60	C	1.57
Cl	0.21	Cl	0.06
Total	99.55		

Composition taken from Grundy & Hassan (1982). †Based on Al + Si = 12 atoms per formula unit.

Differential Thermal Analyses

The cancrinite used in the experiments was crushed to a powder using an agate mortar and pestle. The powdered sample was placed into an Al_2O_3 crucible for differential thermal analyses, which was done by a fully computerized, Netzsch STA 409 EP/3/D Simultaneous TG–DTA equipment capable of producing temperatures ranging from 20 to 1500°C. The sample was heated using a microprocessor-controlled programmer and a data acquisition 414/0 unit consisting of a high-current transformer. The heating thermocouple stage is similar to a two-prong fork. On one prong is placed the empty reference Al_2O_3 crucible, and on the other prong, a weighed amount of finely powdered sample was placed in a similar Al_2O_3 crucible. The thermocouples are made of Pt10%Rh–Pt (Type S). A furnace was placed over the sample and reference crucibles, and both were heated in a controlled manner. The unit was programmed to collect a continuous scan from 20 to 1400°C; other details of data collection are given in Table 2.

Results and Discussion

The thermal data for cancrinite were analyzed using Netzsch software programs. The thermogravimetric (TG) curve, which shows the mass as a function of temperature (T), was corrected for buoyancy effect. The differential thermal analysis (DTA) curve, which shows the temperature difference between a substance and a reference material as a function of T, was corrected for baseline effect. The relationship between change in enthalpy and peak area in the DTA curve was determined by calibration with different standard materials.

Figure 2 shows the TG and DTA curves and their corresponding derivative curves (DTG and DDTA). The latter curves are obtained from the raw (TG, DTA) data using a narrow window for filtering the measured data. The differentiation was done by a modified Golay–Savitzky algorithm of second order. Characteristic data from these curves are summarized in Table 3.

TABLE 2. INFORMATION ON COLLECTION OF TG–DTA DATA ON CANCRINITE

Sample weight	99.70 mg
Heating range	20°C to 1400°C
Heating rate	5°C/min
Furnace atmosphere	Air
TG–DTA sample carrier	Type S
Thermocouples	Pt10%Rh – Pt
Equipment	Netzsch STA 409 EP/3/D

TABLE 3. DATA FROM THE TG–DTG–DTA–DDTA AND XRD ANALYSES OF CANCRINITE

Peaks	Miscellaneous	TG	DTG	DTA	DDTA	XRD	Changes
Peak 1	Endo(–)/Exo(+)?			(–)ve			
	Extr. Onset T	256.4		291.4	284.6		
	Peak T		304.0			~300, *a*, *V*	H_2O (I)
	Extr. End T	405.2		338.3	318.2	Additional peak at 28.5°	
	% Wt. Loss						
	Enthalpy (J/g)						
Peak 2	Endo(–)/Exo(+)?			(–)ve			
	Extr. Onset T	678.3		676.5	672.8		
	Peak T		683.0	695.0		~700, *a*	H_2O (II)
	Extr. End T	861.6		742.2	729.4	Increase in	
	% Wt. Loss	–5.5				Intensities	
	Enthalpy (J/g)			7.90			
Peak 3	Endo(–)/Exo(+)?			(–)ve			
	Extr. Onset T	No	No	837.6	853.9		Phase
	Peak T	Peak	Peak	868.0		~850, *a*, *V*	transition
	Extr. End T			888.2	871.2		Loss
	% Wt. Loss						of
	Enthalpy (J/g)			19.36			supercell
Peak 4	Endo(–)/Exo(+)?			(–)ve			
	Extr. Onset T	924.2		926.9	940.2		
	Peak T		947.0	949.0		~950,	CO_2
	Extr. End T	953.8		963.5	951.1	Increase in	
	% Wt. Loss	–5.3				Intensities	
	Enthalpy (J/g)			117.21			
Peak 5	Endo(–)/Exo(+)?			(–)ve			
	Extr. Onset T	1054.1		1053.2	1061.4		
	Peak T		1065.9	1069.5		~1050, *a*	Cl_2 ?
	Extr. End T	1082.6		1082.3	1070.4		
	% Wt. Loss	–0.7					
	Enthalpy (J/g)			6.24			
Peak 6	Endo(–)/Exo(+)?			(–)ve			
	Extr. Onset T	No	No	1087.8	1093.6		Phase
	Peak T	Peak	Peak	1102.0		~1100, *c*, *V*	transition
	Extr. End T			1111.5	1100.8		? Na–Ca
	% Wt. Loss						disorder
	Enthalpy (J/g)			38.82			
Peak 7	Endo(–)/Exo(+)?			(–)ve			
	Extr. Onset T	No	No	1118.6	1180.0		Phase
	Peak T	Peak	Peak	1199.0			transition
	Extr. End T				1209.0		? Al–Si
	% Wt. Loss						disorder
	Enthalpy (J/g)						
Peak 8	Endo(–)/Exo(+)?			(+)ve			
	Extr. Onset T	No	No		1236.0		
	Peak T	Peak	Peak	1255.0		~1250	Melting
	Extr. End T				1283.0	No peaks	point

All temperatures are expressed in °C. Endo/Exo: endothermic or exothermic; Extr. Onset T: extrapolated onset temperature, *etc.* The XRD column indicates discontinuities in the cell parameters (*a*, *c* and *V*) at the temperature obtained from the XRD experiment.

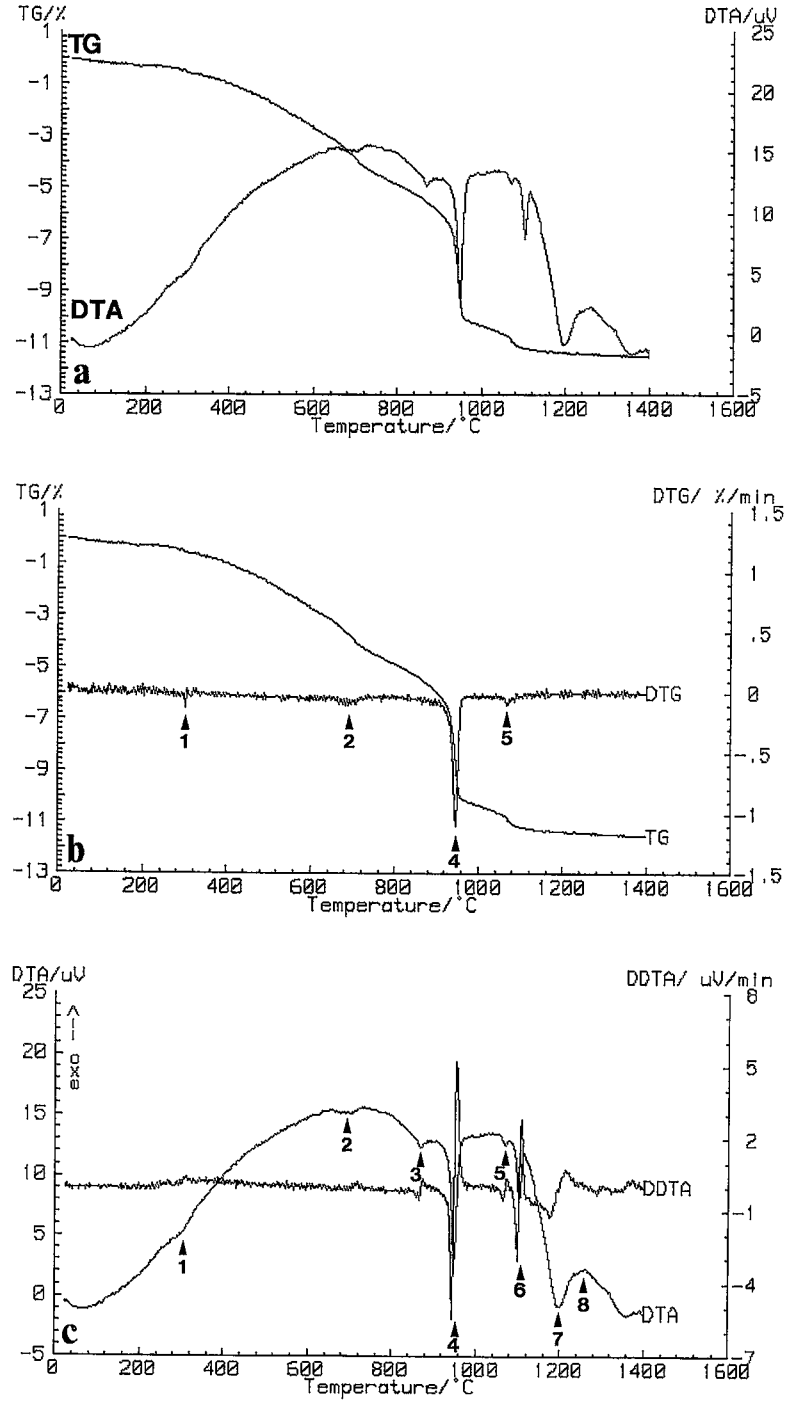

FIG. 2. TG, DTG, DTA, and DDTA curves for cancrinite: (a) TG and DTA curves, (b) TG–DTG curves, showing four peaks that are labeled on the DTG curve, and (c) DTA–DDTA curves, showing eight peaks that are labeled on the DTA curve. In these and subsequent diagrams, corresponding peaks at a particular temperature are given the same number.

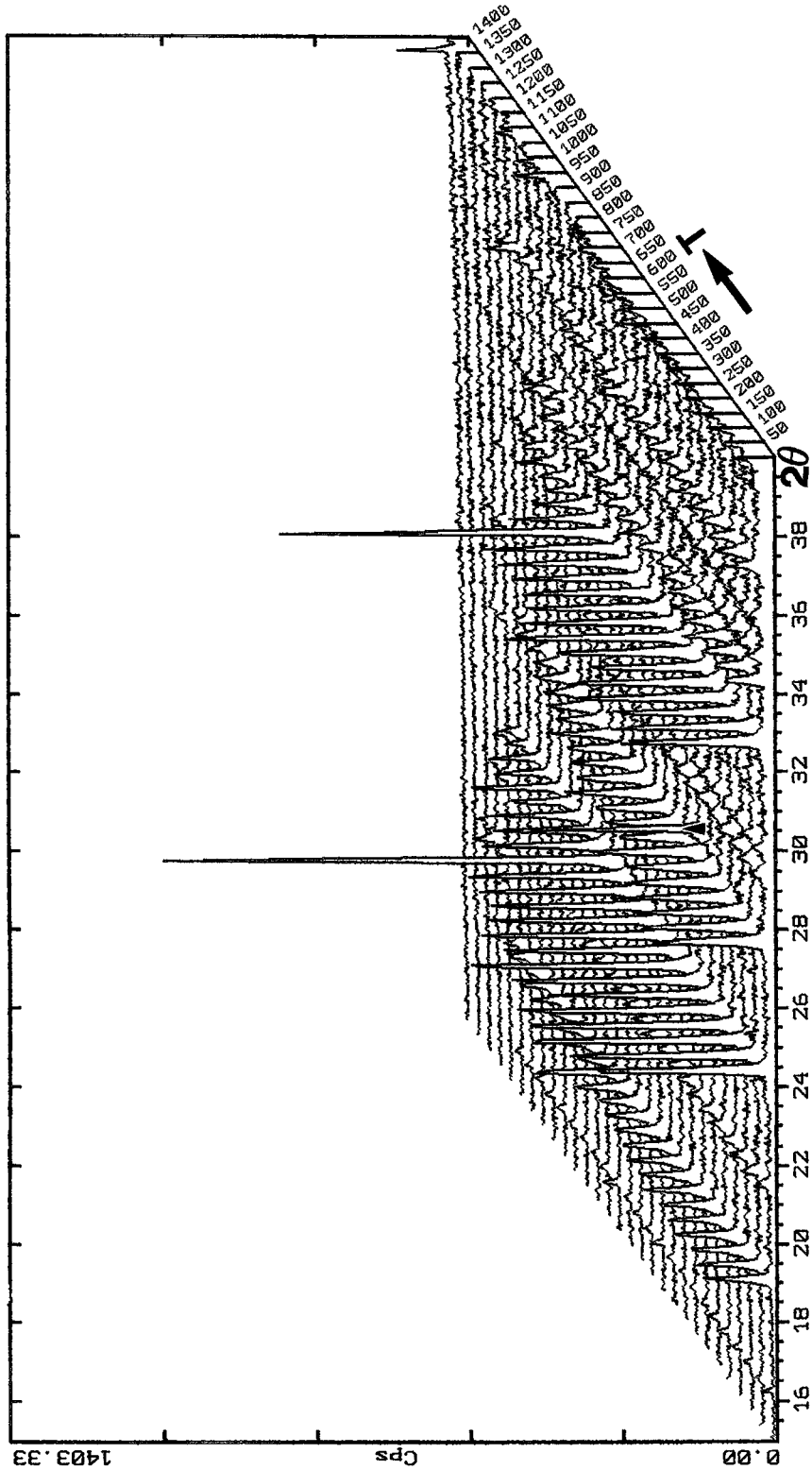

FIG. 3. High-temperature powder XRD data for cancrinite at 20°C (first trace), 50 to 1400°C at intervals of 50°C, and finally at 20°C (beyond the 1400°C trace). Significant increases in intensities are observed at 700°C. Beyond 1200°C, no significant peaks occur. At 300°C, an extra peak occurs at 28.5° (arrow).

From the TG curve, extrapolated onset and end temperatures and the weight percentage (wt.%) loss are obtained for each weight-loss segment (Table 3). The DTG trace gives the temperature where the maximum weight-loss occurs; there are four DTG peaks in the analysis of cancrinite. The DTG peaks 4 and 5 are well defined compared to peaks 1 and 2 (Figs. 2a, b, Table 3). Although visually observable on the DTG curve, peaks 1 and 2 are not obvious on the TG curve, especially peak 1. In fact, a continuous loss of weight occurs over peaks 1 and 2 (Figs. 2a, b) and corresponds to a net loss in weight of about 5.5%. This large continuous loss in weight can be divided into two steps, with losses of about 2.5 wt.% from 20 to about 650°C, and 3.0 wt.% from about 650 to 860°C. Peak 4 shows a loss of weight of about 5.3% over a narrow range in temperature. A small but well-defined weight-loss of about 0.7% is indicated by peak 5 (Figs. 2a, b).

The weight losses shown by the TG curve can be attributed to the escape of H_2O, CO_2, and possibly Cl_2. Initially, H_2O constituted 3.02 wt.%, and CO_2 amounts to 6.6 wt.% (Table 1). If both constituents were completely lost on heating, a total loss of 9.62 wt.% would be expected. The TG curve shows a total weight loss of 11.4%. Because the amount of CO_2 is larger than that of H_2O, the loss of CO_2 will cause the greatest loss in weight, so CO_2 is most likely lost at 947°C (peak 4). According to results of the crystal-structure analysis (Grundy & Hassan 1982), the H_2O is expected to be lost is two steps, each step being associated with a loss of 1.51 wt.%, as indicated by the chemical analyses. Both types of H_2O molecules (I and II) are lost gradually in two stages. H_2O(I) is lost at peak 1, and H_2O(II) is lost at peak 2, corresponding to weight losses of 2.5 and 3.0%, respectively. The total loss of H_2O obtained from the TG curve is 5.5 wt.%. The small weight loss of 0.7% may be attributed to Cl_2, according to results of the chemical analysis (Table 3).

The DTG curve gives the peak temperature as well as extrapolated onset and end temperatures for each peak (Figs. 2a, c, Table 3). The DTA curve also gives the change in enthalpy associated with each peak by computing the area under the peak after calibration. By definition, exothermic change is positive. For each DTA peak, the DDTA curve also gives the onset and end temperatures (Figs. 2a, c, Table 3). Eight peaks are

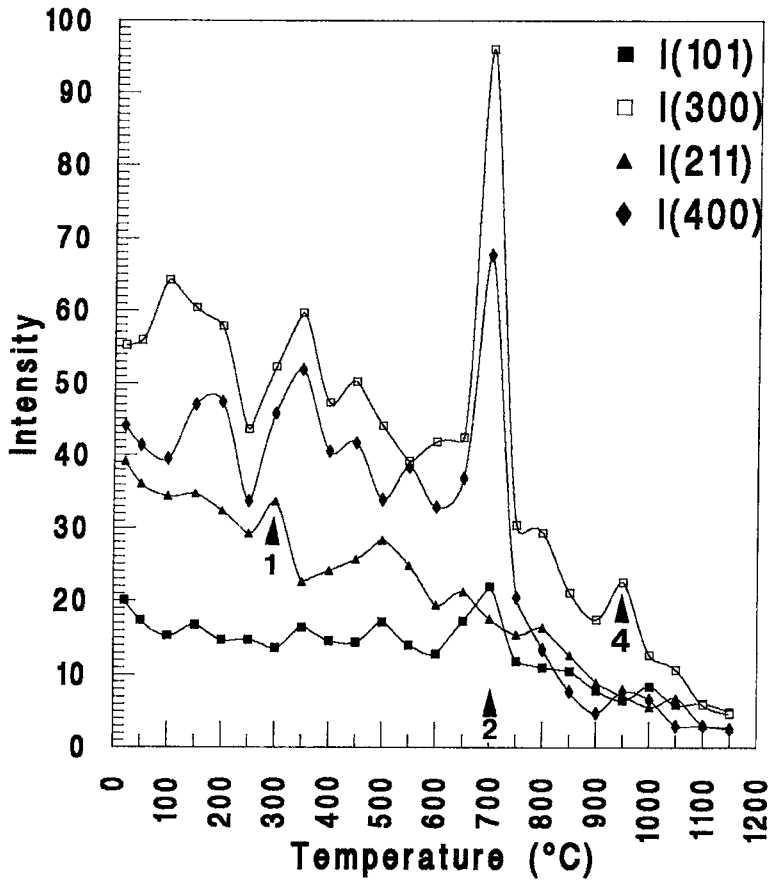

FIG. 4. Variation of intensities of selected reflections with temperature. The arrows point out changes at temperatures that were also detected in the TG–DTA traces.

observed in the DTA curve; peaks 3, 4, 5, 6, 7, and 8 are well defined in both the DTA and DDTA curves, but peaks 1 and 2, although visually detectable, are less obvious (Figs. 2a, c).

Thermal expansion coefficients were also measured for the same sample of cancrinite (Hassan 1996). The raw high-temperature powder XRD data for cancrinite at 20°C, 50 to 1400°C at intervals of 50°C, and finally at 20°C are shown (Fig. 3). At about 1250°C, there are no significant diffraction-peaks. At about 300°C, an extra diffraction-peak occurs (arrow). Significant rises in the intensities of the peaks occur at 700°C.

The variations in intensities of the diffraction peaks with temperature are shown (Fig. 4). The increasing thermal motion of the atoms, brought on by heating, causes the intensities of diffraction peaks to decrease. An increase in diffraction intensity during heating usually indicates a discontinuous change in the structure. In the case of cancrinite, several significant increases in diffraction intensities are observed (Fig. 4).

The refined unit-cell parameters are displayed in Figure 5 (see Hassan 1996). The variations of the percentage changes of unit-cell parameters with temperature were fitted to a polynomial using a least-squares refinement; the resulting relationships are given in the caption to Figure 5. The *c* parameter expands more than the *a* parameter, and the unit-cell parameters increase nonlinearly with increasing temperature. There are changes or discontinuities in the thermal expansion curves that indicate discontinuous changes in the structure (*e.g.*, loss of H_2O, CO_2, *etc.*). These discontinuities are best interpreted in conjunction with the data from differential thermal analyses (Table 3).

The first break (peak 1; Fig. 5) in the cell parameters (*a*, *V*) occurs at 300°C and is accompanied by an additional peak at 28.5° 2θ in the XRD trace (Fig. 3). Peak 1 is associated with loss of H_2O(I), as suggested by the TG–DTA analyses.

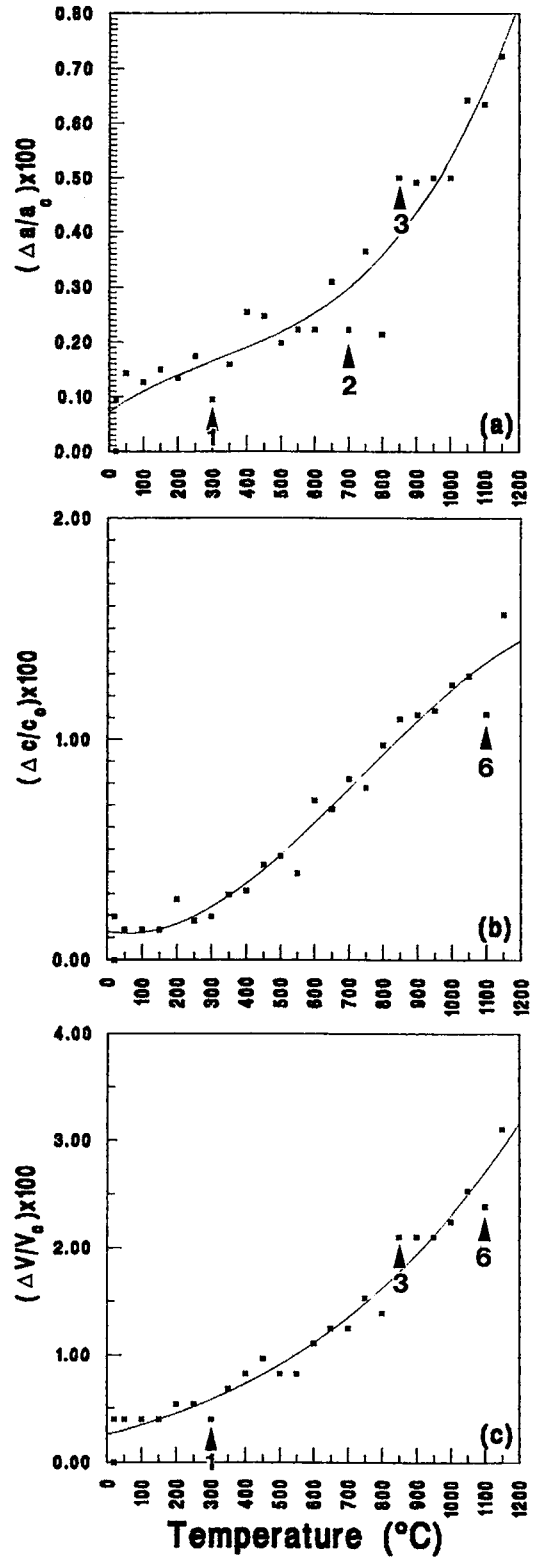

FIG. 5. The variation of the percentage changes in unit-cell parameters with temperature for cancrinite (from Hassan 1996). (a) $\Delta a/a_0$ *versus* T, (b) $\Delta c/c_0$ *versus* T, and (c) $\Delta V/V_0$ *versus* T. The unit-cell parameters increase nonlinearly with temperature. With increasing temperature, the *c* parameter increases more rapidly than the *a* parameter. The arrows point out changes at temperatures that were also detected by TG–DTA traces. The equations of the least-squares fits to the data are: $\Delta a/a_0 = 0.072349 + 4.3507 \times 10^{-4}T - 6.0532 \times 10^{-7}T^2 + 6.3461 \times 10^{-10}T^3$, $r^2 = 0.923$; $\Delta c/c_0 = 0.12772 - 2.8988 \times 10^{-4}T + 2.5439 \times 10^{-6}T^2 - 1.1548 \times 10^{-9}T^3$, $r^2 = 0.966$; $\Delta V/V_0 = 0.25553 + 8.4186 \times 10^{-4}T + 6.4788 \times 10^{-7}T^2 + 5.5398 \times 10^{-10}T^3$, $r^2 = 0.967$.

At 700°C, a discontinuity occurs in *a* (Fig. 5a, peak 2) and is accompanied by a significant increase in the intensities of the 300, 400, and 101 diffraction maxima (Fig. 4, peak 2). This change is associated with loss of H_2O(II), as suggested by the TG–DTA analyses. The H_2O molecules are disordered about the 3-fold axes in the room-temperature structure of cancrinite (Grundy & Hassan 1982; Fig. 1). With the loss of the H_2O molecules, the *a* cell parameter decreases, as would be expected. At this stage, the intensities of the diffraction maxima increase, thus indicating an increase in degree of order in the *a*–*b* plane (001).

An additional discontinuity in *a* and *V* occurs in the thermal expansion curves at 850°C compared to 868°C from the DTA trace (peak 3). At this temperature, no weight loss is detected in the TG–DTG curves. Therefore, at 868°C, a phase transformation occurs in cancrinite. This transformation is associated with the loss of the superstructure, which is related to the ordering of carbonate groups at room temperature (Grundy & Hassan 1982, Hassan & Buseck 1992). Thus, above 868°C, the CO_3 groups are disordered.

There is no change in the thermal expansion curves at 950°C (Fig. 5). However, at 949°C, the most significant change occurs in the TG and DTA curves, corresponding to the loss of CO_2 (peak 4). These changes, however, are reflected in the intensities of the XRD peaks. For example, the intensity of the 300 reflection shows a significant increase at 950°C (Fig. 4, peak 4).

Although no discontinuity in the cell parameters occurs at 1050°C, there is a large change in the *a* parameter from 1000 to 1050°C. However, peak 5 was observed at 1066 and 1070°C in the DTG and DTA traces, respectively. A loss of 0.7 wt.% occurs in the TG trace at 1066°C. There is no obvious explanation for this loss, but it may be associated with loss of Cl_2, as inferred from results of the chemical analyses.

Discontinuities in the *a* and *V* parameters occur at 1100°C (peak 6) and corresponds to the DTA peak 6 that occurs at 1102°C. As there is no change in the TG–DTG curves, another phase transition occurs in the structure of cancrinite at this temperature, and is probably related to disordering of the Na and Ca atoms in the channels of cancrinite.

At 1199°C, a discontinuity occurs only in the DTA trace and is probably related to Al–Si disorder. At 1250°C, the XRD diffraction peaks are insignificant, such that the sample seems to have melted at about 1250°C (Fig. 3). From the DTA data, the melting of cancrinite occurs at 1255°C.

Hassan (1996) proposed a mechanism for the thermal expansion of cancrinite. This model can now be combined with the present data to give a complete description of the thermal behavior of cancrinite. The short Na1–H_2O in the —H_2O(I)——Na1—H_2O(II)—— chain expands to equal the distances between adjacent H_2O molecules in the chain. This causes the Na1 atoms to move toward the plane of the six-membered rings and forces the tetrahedra in the rings to rotate and become more planar. The Na1 atoms then form bonds to all six (O1 and O2) framework oxygen atoms (Fig. 1). These effects cause an increase in both *a* and *c*, and thus an increase in the *c*/*a* ratio. A similar thermal expansion mechanism operates in the sodalite-group minerals, where the six-membered rings and Na–Cl bonds are involved (Hassan & Grundy 1984, 1991). From the present TG–DTA analyses and results of the crystal-structure refinement (Grundy & Hassan 1982), H_2O(I) is apparently lost before H_2O(II), but the loss is continuous. The supercell is destroyed at 868°C, and CO_2 is lost at 949°C. A small weight-loss at 1066°C may mark a loss of Cl_2. The Na and Ca atoms are probably disordered at 1102°C, whereas the Al and Si atoms are probably disordered at 1199°C. Finally, melting of cancrinite occurs at 1255°C.

This study clearly shows the advantages of using the combined methods of high-temperature XRD analyses coupled with TG–DTG analyses; if only a single method of analysis is chosen, studies are prone to erratic interpretations. For example, in Figure 5, the inserted arrows point out breaks in the thermal expansion curves that were also detected in the TG–DTA curves. Without the latter information, other peaks could erroneously be inferred to be significant in the thermal expansion curves.

Acknowledgements

The referees, Drs. R.N. Abbott and F.F. Foit, Jr., and the Associate Editor, Dr. J.M. Hughes are thanked for useful comments on this manuscript. This work was financially supported by the University of Kuwait in the form of a Research Grant (SG–038). The DTA–TG and XRD measurements were made in the Mineralogical Laboratory, Department of Geology, University of Kuwait.

References

Grundy, H.D. & Hassan, I. (1982): The crystal structure of a carbonate-rich cancrinite. *Can. Mineral.* **20**, 239-251.

Hassan, I. (1996): Thermal expansion of cancrinite. *Mineral. Mag.* **60**, (in press).

_____ & Buseck, P.R. (1992): The origin of the superstructure and modulations in cancrinite. *Can. Mineral.* **30**, 49-59.

_____ & Grundy, H.D. (1984): The crystal structures of sodalite-group minerals. *Acta Crystallogr.* **B40**, 6-13.

_____ & _____ (1991): The crystal structure and thermal expansion of tugtupite, $Na_8[Al_2Be_2Si_8O_{24}]Cl_2$. *Can. Mineral.* **29**, 385-390.

Received January 22, 1996, revised manuscript accepted April 8, 1996.